processes

MDPI

Article

ECG Identity Recognition Based on Feature Reuse Residual Network

Zhengqiang Yang [1], Linyue Liu [1], Ning Li [2,*] and Junwei Tian [3]

[1] School of Computer Science and Engineering, Xi'an Technological University, Xi'an 710021, China; yangzhengqiang@xatu.edu.cn (Z.Y.); liulinyue@st.xatu.edu.cn (L.L.)
[2] School of Electrical Engineering, Xi'an University of Technology, Xi'an 710048, China
[3] School of Mechatronic Engineering , Xi'an Technological University, Xi'an 710021, China; junweitian@xatu.edu.cn
* Correspondence: lining83@xaut.edu.cn; Tel.: +86-137-7202-3927

Abstract: With the increasing demand for security and privacy, identity recognition based on the unique biometric features of ECG signals is gaining more and more attention. This paper proposes a feature reuse residual network (FRRNet) model to address the problem that the recognition accuracy of conventional ECG identification methods decreases with the increase in the number of testing samples at different moments or in different heartbeat cycles. The residual module of the proposed FRRNet model uses the adding layers of max pooling (MP) and average pooling (AP), and the proposed model splices the deep network with the shallow network to reduce noise extraction and enhance feature reuse. The FRRNet model is tested on 20 and 47 subjects under the MIT-BIH dataset, and its recognition accuracy is 99.32% and 100%, respectively. Additionally, the FRRNet model is tested on 50 and 87 subjects under the PhysioNet/Computing in Cardiology Challenge 2017 (CinC_2017) dataset, and its recognition accuracy is 94.52% and 93.51%, respectively. A total of 20 subjects are taken from the MIT-BIH and the CinC_2017 datasets for testing, and the recognition accuracy is 98.97%. The experimental results show that the FRRNet model proposed in this paper has high recognition accuracy, and the recognition accuracy is not greatly affected when the number of individuals increases.

Keywords: ECG; identification; FRRNet; max pooling; average pooling; feature reuse

Citation: Yang, Z.; Liu, L.; Li, N.; Tian, J. ECG Identity Recognition Based on Feature Reuse Residual Network. *Processes* **2022**, *10*, 676. https://doi.org/10.3390/pr10040676

Academic Editors: Alex Shenfield, Marcos Rodrigues and Bernardi Pranggono

Received: 23 February 2022
Accepted: 28 March 2022
Published: 30 March 2022

1. Introduction

With the development of technology and the increase in security requirements, traditional methods such as keys and passwords no longer meet people's needs. Authentication systems with unique biometric features have come into the public eye. For example, facial features [1,2], fingerprints and palmprints [3,4], iris [5,6], voice [7], etc., which are secure and easy to use, have better prospects than the classical methods. However, these biometric authentication methods are easily replicated and prone to change over time. In recent years, biometric authentication systems based on electrocardiographic (ECG) signals have been increasingly used. Compared with other biological characteristics, ECG signals are not only difficult to duplicate and disturb, but also have more advantages than the existing methods in terms of security, privacy and stability [8–15]. Moreover, all living individuals present ECG signals, which have the inherent vivo detection function.

In recent years, identity recognition methods based on ECG signals have been widely used. It is feasible to use machine learning for identity recognition. S. A. Israel et al. [16] proposed a recognition method using 15 feature points, Wilks' lambda for feature selection and linear discriminant analysis (LDA) for dimensionality reduction and classification, and the recognition accuracy was 90%. S.-L. Lin et al. [17] used the root-mean-square (RMS) value, nonlinear Lyapunov exponent and correlation dimension for ECG signal analysis and used the support vector machine (SVM) classifier for identity recognition,

and the recognition accuracy was over 80%. Belgacem et al. [18] proposed a system based on discrete wavelet transform (DWT) to extract features and random forest to achieve authentication, concluding that the system could achieve high accuracy and low false positive rates. Zokaee and Faez [19] proposed a multi-modal recognition system based on palmprints and ECG biometric features, using the mel-frequency cepstral coefficient (MFCC) algorithm for ECG feature extraction and principal component analysis (PCA) for palmprint feature extraction, and finally using the k-nearest neighbour (KNN) classifier to achieve classification, and the recognition accuracy was 94.7%. El_Rahman et al. [20] proposed a multi-modal biometric system based on the MIT-BIH database and the FVC database, where self-organising feature map-neural network (SOM-NN), fuzzy logic (FL) and LDA were used in parallel, and the recognition accuracy was 98.5%. Although the above methods achieved high accuracy, they did not present the significantly improved accuracy after optimising the parameters up to a certain limit. Moreover, the training efficiency of complex models is low, so it is difficult to use a large amount of data to repeat the training models, and prone to cause overfitting after using a small amount of data to repeat the training. Complex models only rigidly record the features of the training set and tend to preserve noise as features.

With the proposal of deep learning methods such as neural networks, more and more researchers have applied deep learning methods to ECG identification. The neural-network-based ECG signal identification method is characterised by faster testing and higher recognition accuracy. In the further development of neural networks, problems such as overfitting have been solved, and this method is compatible with the development of artificial intelligence in terms of sustainability. Belo, David et al. [21] used the recurrent neural network (RNN) model of the non-benchmark system network to output a score based on the predicted error, using the temporal convolutional neural network (TCNN) for the non-benchmark systems, giving a score according to the output of the last layer. The two scores were calculated and fed to the relative score threshold classifier (RSTC) and the recognition accuracy was 96%. Liu, Xin et al. [22] proposed a two-level fusion PCANet deep recognition network that achieved a recognition accuracy of over 95% on the MIT-BIH dataset. Dang, Hao et al. [23] used network models of CNN, multi-scale CNN and multi-scale CNN plus residual block for identity recognition on the MIT-BIH dataset, and the overall recognition accuracy was 93.41%, 96.83% and 97.03%, respectively. Mohamed Hammad et al. [24] improved the ResNet model and added the attention module, and achieved recognition accuracy of 98.85% and 99.27% on the two datasets of PTB and CYBHI, respectively. Chayma Yaacoubi et al. [25] achieved the recognition accuracy of 94% on the TROIKA database using a combination of CNN and RNN. Yue Zhang et al. [26] improved the multi-scale CNN by adding the residual module and combining the nearest neighbour classifier and SVM to achieve classification recognition, and the average recognition accuracy was 97.7% and 98.7%, respectively. Ranjeet Srivastva et al. [27] combined ResNet, DenseNet and transfer learning. First, the ECG signals from datasets of PTB and CYBHI were converted into 2D images, then the images were input into each model for training, using cascade fusion of features from each model. The result of the fusion was a feature vector representing the weight of each class. The overall recognition accuracy was 99.66%. This method increased the data conversion steps and used multiple models for training, which increased the memory consumption.

In summary, although all of these research methods have achieved high recognition accuracy, they required higher requirements in practical application to ensure that the systems and equipment applied to the ECG identification methods provided essential security. In most studies, the time interval between the ECG signals in the training and testing sets was short or fell into the same heartbeat cycle, which resulted in higher recognition accuracy. However, in practical applications, the time interval between the heartbeat during recognition and the recording of the ECG signals in the training set differs significantly. In order to serve more users, the robustness of the ECG identification system needs to be further improved.

Based on the above problems and analysis, the FRRNet model, an improved model based on ResNet18, is proposed in this paper. Firstly, the original signals are pre-processed using the 6-layer wavelet transform. Then, features are extracted from the processed data to facilitate heartbeat segmentation. Finally, the segmented training and testing sets are input into the identity recognition system based on the FRRNet model.

The FRRNet model proposed in this paper has two features. (1) The output of the max pooling (MP) layer is added to that of the average pooling (AP) layer at the short circuit, which is expected to preserve the strong features and reduce the impact of mistaking noise for features through AP. (2) In order to enhance the robustness of the FRRNet model, the output results of the shallow network are combined with those of MP and AP to strengthen feature reuse. The FRRNet model proposed in this paper aims to increase the number of feature points to improve the recognition accuracy while reducing the impact of the high memory consumption of the DenseNet model during training to a certain extent.

The rest of this paper is organised as follows. Section 2 introduces the dataset and the network model. Section 3 describes the pre-processing, the segmentation of the dataset and the identification methods. Section 4 compares the FRRNet model with other models, illustrates the experimental results and discusses them. Section 5 presents the conclusions.

2. Related Work

2.1. Introduction to the Dataset

This study used the MIT-BIH dataset [28] and the PhysioNet/Computing in Cardiology Challenge 2017 [29] (CinC_2017) dataset for ECG identification. The two datasets contain both normal and abnormal ECG signals, which is in line with the heartbeat situation of the actual population. Compared with other datasets, the noise of the CinC_2017 dataset is louder, which has a greater impact on ECG signal identification, consistent with the actually obtained heartbeat records. In this study, one channel record from each subject in the MIT-BIH dataset was selected and 87 ECG signals from the CinC_2017 dataset were extracted; thus two datasets were used for ECG identification.

Recordings in the MIT-BIH dataset were obtained from limb leads (MLII) as well as chest leads (V1, V2, V4 or V5), recording subjects' ECG signals for 30 min. In this paper, the ECG signal records of each subject with a duration of 1 min were selected for experiments. Recordings in the CinC_2017 dataset were acquired by AliveCor single-channel ECG devices, with two electrodes maintained in each hand to form an I-lead (LA-RA) equivalent ECG, which recorded ECG signals for an average of 30 s.

2.2. Introduction to ResNet Neural Network

The ResNet neural network [30] was proposed to solve the problems of network optimization such as gradient disappearance or explosion when the network layers were deepened. The residual module contains two, three or more layers, as shown in Figure 1. The formula for the residual layer is as follows:

$$F(x) = H(x) - x \tag{1}$$

where $H(x)$ refers to the desired basic mapping; $F(x)$ refers to the stacked non-linear layer fitting; and x refers to the output of the upper layer.

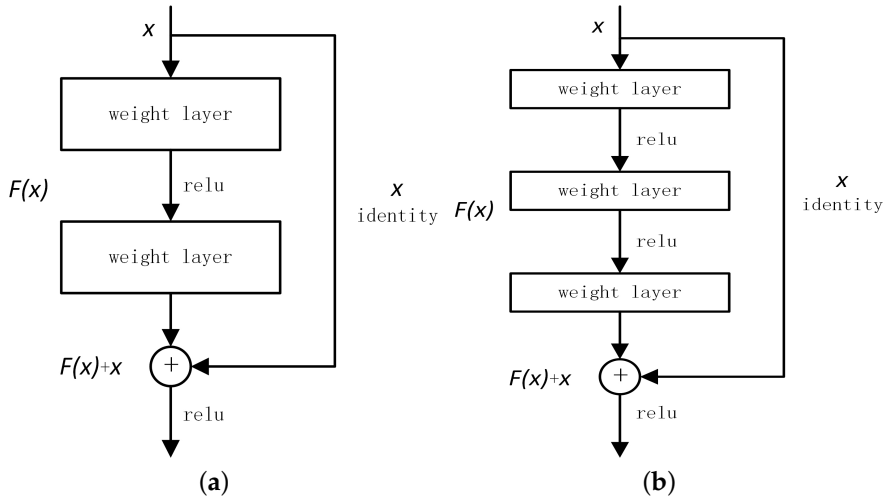

Figure 1. ResNet model residual module: (**a**) the residual module contains two layers; (**b**) the residual module contains three layers.

3. Methods

This section describes the methods of preprocessing the original ECG signals and of extracting their features, and introduces the FRRNet proposed in this paper, an improved ResNet network. The system flow diagram for this paper is shown in Figure 2.

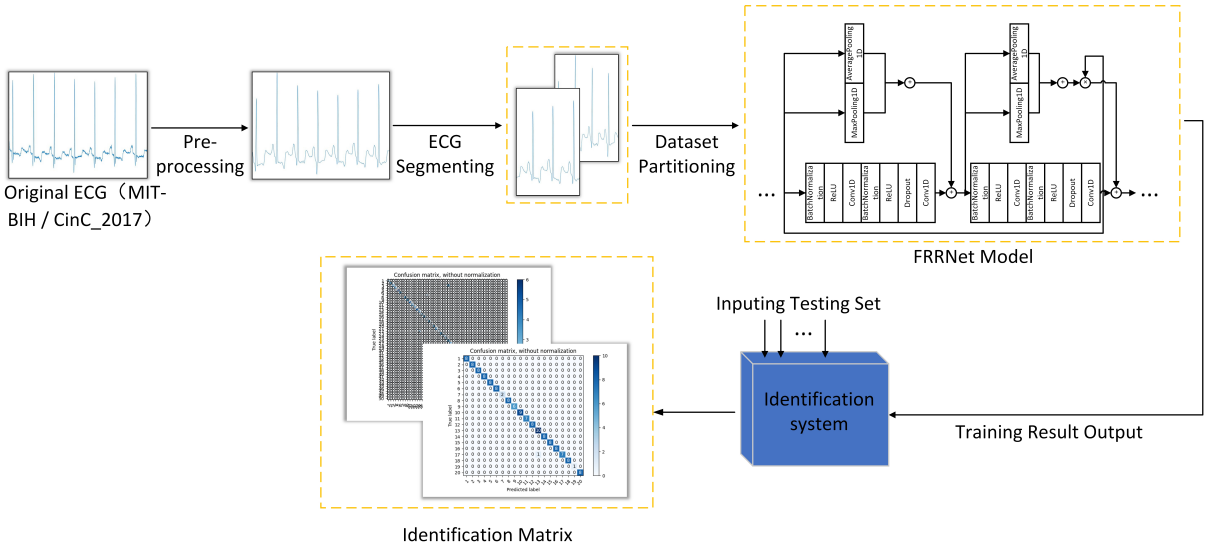

Figure 2. System flow diagram.

3.1. Pre-Processing

The pre-processing flow of the original ECG signals is shown in Figure 3. In this paper, the high-frequency noise and baseline drift were removed by 6-layer wavelet transform [31–33]. The original and pre-processed ECG signals in the MIT-BIH dataset and the original and pre-processed ECG signals in the CinC_2017 dataset are shown in Figure 4.

The wavelet transform decomposed the signals into low- and high-frequency components in turn and then reconstructed them, as shown in Figure 3. The ECG signal *f(n)* passed through the low-frequency filter *h(n)* and was then down-sampled to obtain the first-level approximation coefficients *c*. In the same way, ECG signals passed through the high-frequency filter *g(n)* and were then down-sampled to obtain the first-level detail coefficients *d*. The wavelet transform equation is shown in Formulas (2) and (3):

$$c_{j+1}(n) = \sum_m c_j(m)h(m-2n) \tag{2}$$

$$d_{j+1}(n) = \sum_m c_j(m)g(m-2n) \tag{3}$$

The reconstruction formula is shown in Formula (4):

$$c_j(n) = \sum_m c_{j+1}(m)h(n-2m) + d_{j+1}(m)g(n-2m) \tag{4}$$

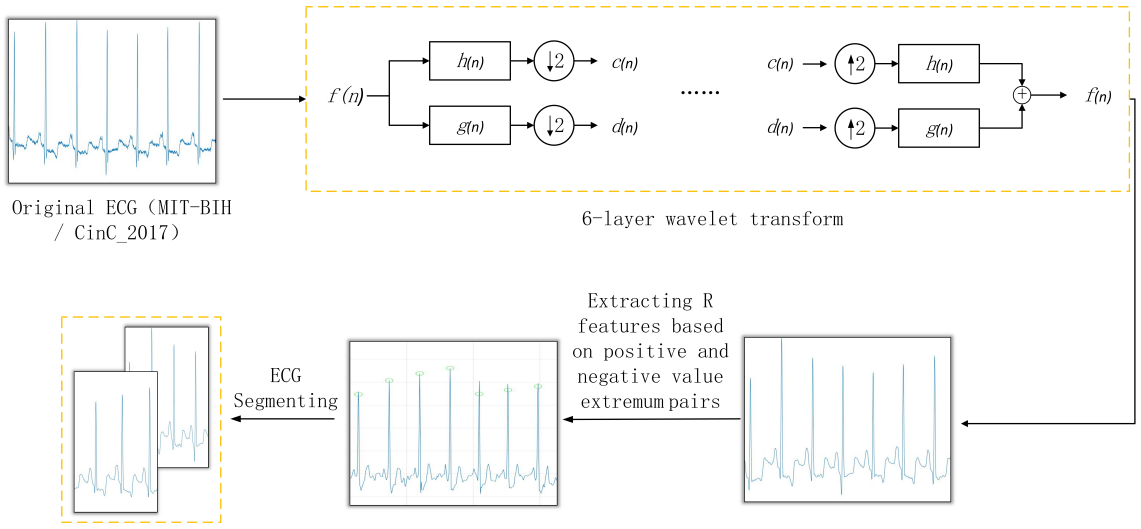

Figure 3. Pre-processing flow diagram.

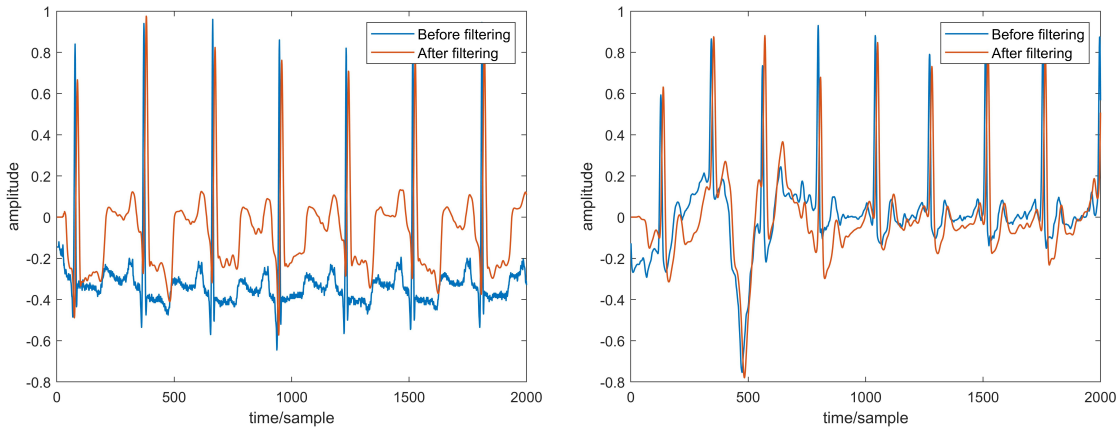

Figure 4. Original and pre-processed ECG signal diagrams of the datasets: (**a**) Original and pre-processed ECG signal diagram of the MIT-BIH dataset; (**b**) Original and pre-processed ECG signal diagram of the CinC_2017 dataset.

3.2. Heartbeat Segmentation

In order to segment heartbeat, we performed feature extraction on the processed data. For ECG signal feature extraction, firstly, we calculated the positive and negative maximum pairs to determine the wave peaks and troughs. Secondly, we determined the R-wave peak through the positive and negative extremum pairs over the threshold point. Finally, we deleted the multi-detection R-wave feature points and compensated for the missed R-wave feature points [34,35]. In this study, the segmentation was carried out according to R-wave feature points. In order to obtain the heartbeat signals closer to the actual detection situation in the identity recognition system, the heartbeat segments with the length of

800 sample points were uniformly selected as a set of data ensuring that the data contained the uncertain starting points and the number of the heartbeat cycles. The segmentation diagram of 800 sample points is shown in Figure 5.

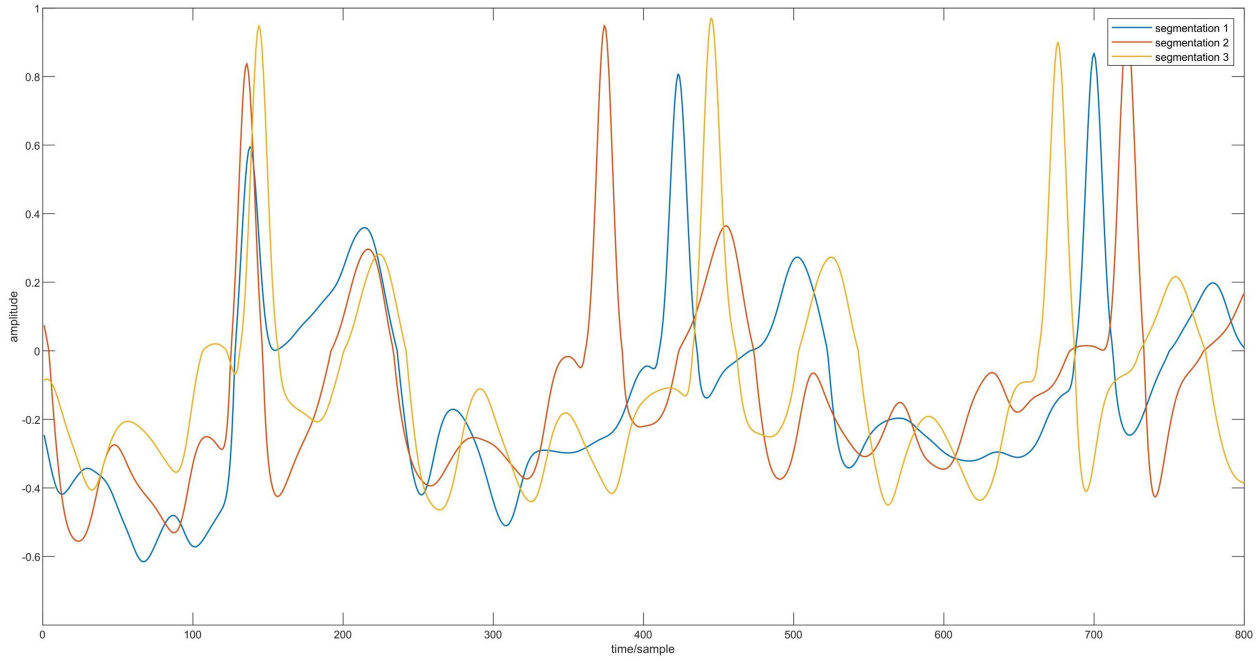

Figure 5. The segmentation diagram of 800 sample points.

3.3. Feature Reuse Residual Network

In this paper, the segmented ECG signals were input into the residual module by selecting the direct down-sampling ResNet18 model (DRN18), the MP ResNet18 model (MRN18) and the AP ResNet18 model (ARN18). Additionally, the segmented ECG signals were also input into the FRRNet model, an improved ResNet18 model proposed in this paper. By comparing these four models, it was concluded that the FRRNet model proposed in this paper had higher recognition accuracy, stronger robustness and generalisation ability. Compared with the DenseNet model, the FRRNet model reduced the memory consumption during training by reducing the number of branches from the shallow to the deep network. The residual module diagrams of DRN18, MRN18 and ARN18 are shown in Figure 6. The residual module diagram of FRRNet is shown in Figure 7. The structure of the FRRNet model is shown in Table 1. The parameters of the FRRNet model are shown in Table 2.

The MP residual module preserved the features and reduced the impact of the offset of the estimated value caused by parameter errors in the convolution layer. The AP residual module preserved the background and reduced the impact of the increase in estimated value variance caused by the limitation of domain size. However, there were some problems with the residual module in the ResNet18 model using either direct down-sampling or MP or AP. When selecting direct down-sampling, the recognition accuracy of the model was low and it could not meet the practical requirements. When selecting MP, there was a possibility that noise was extracted as feature points, thus reducing the recognition accuracy. When selecting AP, the model focused on the background and blurred the features, which also reduced the recognition accuracy. The recognition accuracy of the three ResNet18 models tested under the two datasets used in this paper differed significantly, indicating that the generalisation ability of the ResNet18 models could be further improved.

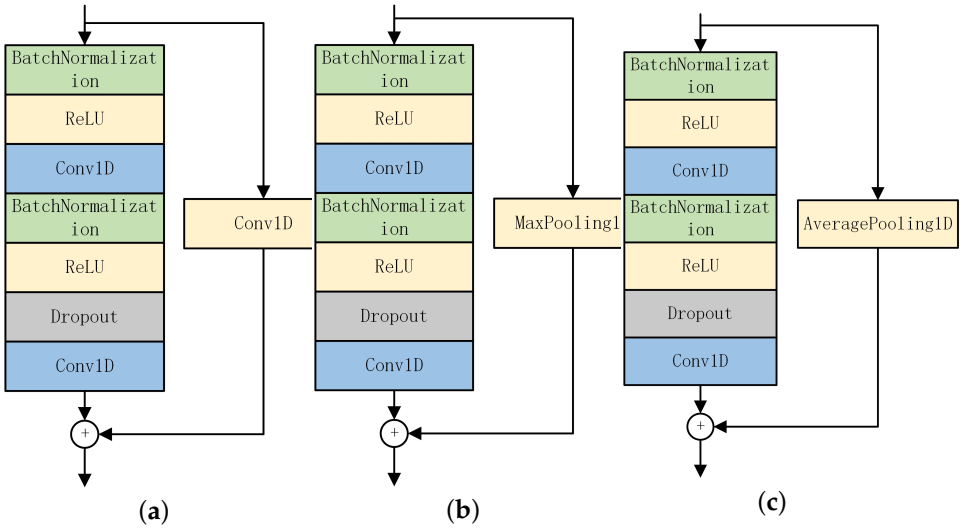

Figure 6. Convolutional neural network model structure: (**a**) DRN18 residual module structure; (**b**) MRN18 residual module structure; (**c**) ARN18 residual module structure.

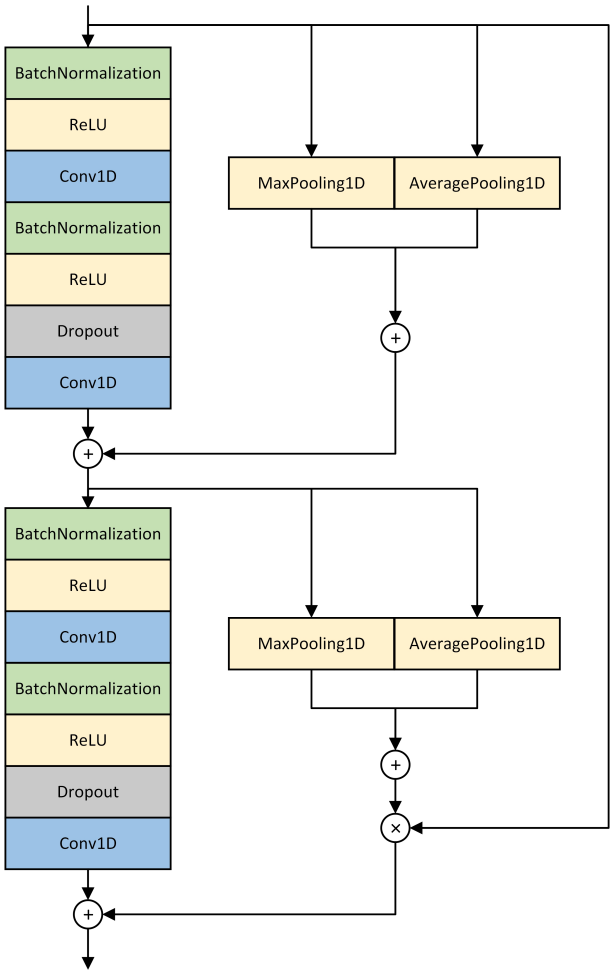

Figure 7. FRRNet residual module structure.

Table 1. Network model structure.

Layer Name	Output Size	Layer			
conv1 (Conv1D)	(None, 800, 32)	1 × 32, 32, stride 1			
conv2_x (Conv1D)	(None, 800, 32)	1 × 32, 32	1 × 2, max_pooling1d, stride 1	1 × 2, average_pooling1d, stride 1	
conv3_x (Conv1D)	(None, 400, 32)	1 × 32, 32	1 × 2, max_pooling1d, stride 2	1 × 2, average_pooling1d, stride 2	1 × 32, 32
conv4_x (Conv1D)	(None, 400, 64)	1 × 32, 64	1 × 2, max_pooling1d, stride 1	1 × 2, average_pooling1d, stride 1	
conv5_x (Conv1D)	(None, 200, 64)	1 × 32, 64	1 × 2, max_pooling1d, stride 2	1 × 2, average_pooling1d, stride 2	1 × 32, 64
conv6_x (Conv1D)	(None, 200, 128)	1 × 32, 128	1 × 2, max_pooling1d, stride 1	1 × 2, average_pooling1d, stride 1	
conv7_x (Conv1D)	(None, 100, 128)	1 × 32, 128	1 × 2, max_pooling1d, stride 2	1 × 2, average_pooling1d, stride 2	1 × 32, 128
conv8_x (Conv1D)	(None, 100, 256)	1 × 32, 256	1 × 2, max_pooling1d, stride 1	1 × 2, average_pooling1d, stride 1	
conv9_x (Conv1D)	(None, 50, 256)	1 × 32, 256	1 × 2, max_pooling1d, stride 2	1 × 2, average_pooling1d, stride 2	
	(None, 256)	Global_average_pooling1d, 87-d fc, softmax			

Table 2. Network model parameters.

epoch	300
activation	ReLU
dropout	0.5
batch size	16
learning rate	0.001

To illustrate that the FRRNet model proposed in this paper could better solve the problems of the three ResNet18 models mentioned above, the ECG signal sequences of 50 sample points from the number 100 subject in the MIT-BIH dataset were selected and are shown in Table 3. Red marks in Table 3 denote noise and blue marks denote feature points. Using the filter with the length of 8, we compared the data processed by MP or AP with those processed by MP + AP. With mathematical calculation, this showed that MP + AP was better able to avoid the above problems, as shown in Table 4. The ECG signal sequence in Table 4 was the same as that in Table 3.

Table 3. Partial ECG signal sequence of the number 100 subject (Red marks denote noise and blue marks denote feature points).

No.	**1**	**2**	**3**	**4**	**5**	**6**	**7**	**8**	**9**	**10**
Points	0.730	0.735	0.734	0.730	0.722	0.711	0.698	0.683	0.665	0.641
No.	**11**	**12**	**13**	**14**	**15**	**16**	**17**	**18**	**19**	**20**
Points	0.609	0.569	0.520	0.463	0.399	0.331	0.261	0.193	0.129	0.072
No.	**21**	**22**	**23**	**24**	**25**	**26**	**27**	**28**	**29**	**30**
Points	0.022	−0.019	−0.054	−0.083	−0.106	−0.126	−0.143	−0.156	−0.167	−0.175
No.	**31**	**32**	**33**	**34**	**35**	**36**	**37**	**38**	**39**	**40**
Points	−0.181	−0.183	−0.183	−0.182	−0.179	−0.177	−0.178	−0.183	−0.197	−0.221
No.	**41**	**42**	**43**	**44**	**45**	**46**	**47**	**48**	**49**	**50**
Points	−0.258	−0.309	−0.376	−0.456	−0.541	−0.619	−0.673	−0.684	−0.629	−0.482

Table 4. Calculation results of the three methods.

MP	0.735	0.735	0.734	0.730	0.722	0.711	0.698	0.683	0.665	0.641
	0.609	0.569	0.520	0.463	0.399	0.331	0.261	0.193	0.129	0.072
	0.022	−0.019	−0.054	−0.083	−0.106	−0.126	−0.143	−0.156	−0.167	−0.175
	−0.177	−0.177	−0.177	−0.177	−0.177	−0.177	−0.178	−0.183	−0.197	−0.221
	−0.258	−0.309	−0.376	−0.456	−0.482	−0.482	−0.482	−0.482	−0.482	−0.482
AP	0.718	0.710	0.698	0.682	0.662	0.637	0.606	0.569	0.525	0.474
	0.418	0.358	0.296	0.234	0.174	0.117	0.065	0.019	−0.021	−0.055
	−0.083	−0.107	−0.126	−0.142	−0.155	−0.164	−0.171	−0.176	−0.178	−0.180
	−0.181	−0.183	−0.188	−0.197	−0.213	−0.237	−0.273	−0.318	−0.372	−0.432
	−0.490	−0.536	−0.558	−0.583	−0.605	−0.617	−0.617	−0.598	−0.556	−0.482
MP + AP	1.453	1.445	1.432	1.412	1.384	1.348	1.304	1.252	1.190	1.115
	1.027	0.927	0.816	0.697	0.573	0.448	0.326	0.212	0.108	0.017
	−0.061	−0.126	−0.180	−0.225	−0.261	−0.290	−0.314	−0.332	−0.345	−0.355
	−0.358	−0.360	−0.365	−0.374	−0.390	−0.414	−0.451	−0.501	−0.569	−0.653
	−0.748	−0.845	−0.934	−1.039	−1.087	−1.099	−1.099	−1.080	−1.038	−0.964

The results in Table 4 show that after the ECG signal sequence was processed by MP, the sequence trend changed to a certain extent, retaining the feature point of 0.735, but failed to remove the noise of −0.177. After the AP processing, the motion trend of the data sequence was better retained, but the feature points were blurred to some extent. In contrast, the MA adopted in this paper not only maintained the motion trend of the data sequence but also ensured that the sequence trend of the processed ECG signals was similar to that of the original signals, and some sample points contained feature signals, reducing the impact of the blurred AP features. Therefore, this method better extracted features, avoided noise with a greater probability and better maintained the desired motion trend, which had a positive effect on identity recognition and matching and improved the robustness of the original models.

4. Experiment and Analysis

This paper carried out identity training and testing based on the MIT-BIH and the CinC_2017 datasets. In the MIT-BIH dataset, 47 subjects have a total of 808 sets of ECG signal sequences, of which 523 is the training set and 285 is the testing set. In the CinC_2017 dataset, 87 subjects have a total of 532 sets of ECG signal sequences, of which 317 comprise the training set and 215 comprise the testing set. To evaluate the performance of the model proposed in this paper on the large samples of the dataset of loud-noise ECG signals, the two datasets were designed as three testing sets for identity recognition. The testing set in Group 1 for each subject contained an ECG signal sequence to test the accuracy of the FRRNet model proposed in this paper for identity recognition. The testing set in Group 2 for each subject contained several ECG signal sequences to verify the robustness of ECG signal identification at different moments and with different numbers of ECG signal sequences. Group 3 was a mixture of 20 subjects' data taken from the MIT-BIH and the CinC_2017 datasets, including the normal heartbeat records of 8 subjects and the arrhythmia heartbeat records of 1 subject in the MIT-BIH dataset, as well as the normal heartbeat records of 10 subjects and the arrhythmia heartbeat records of 1 subject in the CinC_2017 dataset. In this paper, in order to verify that the proposed FRRNet model maintained good performance despite the increase in the number of subjects, tests were conducted on the MIT-BIH dataset with 20 and 47 subjects, and on the CinC_2017 dataset with 50 and 87 subjects.

The preprocessing in this paper was implemented based on MATLAB2021a. The improved ResNet network model FRRNet was achieved based on Python 3.6. The operating system was the 64-bit Windows operating system with 8.00 GB of RAM and an Intel(R) Core(TM) i7-5500U CPU @ 2.40 GHz processor.

In this paper, the performance of the two systems was evaluated by four metrics: *Accuracy* (Acc), *Sensitivity* (Sen), *Precision* (Pre) and F_1, which were calculated by the following equations.

$$Accuracy = \frac{TP + TN}{TP + FP + TN + FN} \tag{5}$$

$$Sensitivity = \frac{TP}{TP + FN} \tag{6}$$

$$Precision = \frac{TN}{FP + TN} \tag{7}$$

$$F_1 = \frac{2 \times Sensitivity \times Precision}{Sensitivity + Precision} \tag{8}$$

where *TP* (true positive) is the number of samples that are actually identified as positive, *TN* (true negative) is the number of samples that are actually identified as negative, *FP* (false positive) is the number of samples mistakenly identified as positive that are actually negative, and *FN* (false negative) is the number of samples mistakenly identified as negative that are actually positive. Sensitivity and precision are more relevant performance criteria than accuracy in ECG identity recognition due to the great differences between different categories. F_1 is a metric used to measure the accuracy of a multi-label classification model. In this paper, the total Pre and Sen for all categories were calculated first and then F_1 was calculated.

4.1. Identification Results Based on the MIT-BIH Dataset

For Group 1 of the testing set, Acc, Sen and Pre of the FRRNet model proposed in this paper achieved up to 100%, and F_1 was 1. Compared with the models using direct down-sampling, MP and AP, Acc was improved by 4.26%, 2.13% and 4.26%, respectively. Sen was improved by 4.26%, 2.13% and 4.26%, respectively. Pre was improved by 6.38%, 3.19% and 6.38%, respectively, and F_1 was improved by 0.0533, 0.0266 and 0.0533, respectively. For Group 2 of the testing set, Acc, Sen and Pre of the FRRNet model achieved up to 100%, and F_1 was 1. Compared with the models using direct down-sampling, MP and AP, Acc was improved by 1.6%, 1.28% and 4.26%, respectively. Sen was improved by 3.66%, 2.66% and 4.26%, respectively. Pre was improved by 3.56%, 3.87% and 6.38%, respectively, and F_1 was improved by 0.0361, 0.0327 and 0.0533, respectively, as shown in Table 5. The model proposed in this paper has some advantages compared with other methods, and the recognition accuracy was improved by 0.7–5%, as shown in Table 6. It can be seen from the accuracy diagram that the FRRNet model and the ARN18 model, compared with other models, tended to stabilise faster, as shown in Figure 8. The FRRNet model performed well on the two groups of testing sets of 20 and 47 subjects selected from the MIT-BIH dataset. Additionally, for 20 subjects, Acc was 99.32%, Sen 99.38% and Pre 99.55%, and F_1 was 0.9946. Moreover, the recognition accuracy did not decrease due to the increase in the number of testing sets, as shown in Table 7. The matrix of results for each type of identification is shown in Figure 9. In summary, the FRRNet model proposed in this paper had good performance in terms of faster convergence, higher accuracy, better robustness and less impact on accuracy when increasing the dataset on the MIT-BIH dataset.

Table 5. Identification accuracy results.

Model	Set	Acc	Sen	Pre	F_1	Set	Acc	Sen	Pre	F_1
DRN18	Group 1	95.74%	95.74%	93.62%	0.9467	Group 2	98.40%	96.34%	96.44%	0.9639
MRN18	Group 1	97.87%	97.87%	96.81%	0.9734	Group 2	98.72%	97.34%	96.13%	0.9673
ARN18	Group 1	95.74%	95.74%	93.62%	0.9467	Group 2	95.74%	95.74%	93.62%	0.9467
FRRNet	Group 1	**100%**	**100%**	**100%**	**1**	Group 2	**100%**	**100%**	**100%**	**1**

Table 6. Comparison of the proposed model with other methods.

Reference	Method	Dataset	Acc
El_Rahman [20]	AUC for sequential multi-mode systems	MIT-BIH	98.5%
Belo [21]	TCNN	MIT-BIH	96%
Liu, Xin [22]	Two-level PCANet	MIT-BIH	95%
Ding, Ling-Juan [26]	Improved AlexNet	MIT-BIH	99.27%
Our work	FRRNet	MIT-BIH	**100%**

Table 7. Comparison of identification results for 20 and 47 subjects.

Number of Subjects	Acc	Sen	Pre	F_1
20	99.32%	99.38%	99.55%	0.9946
47	100%	100%	100%	1

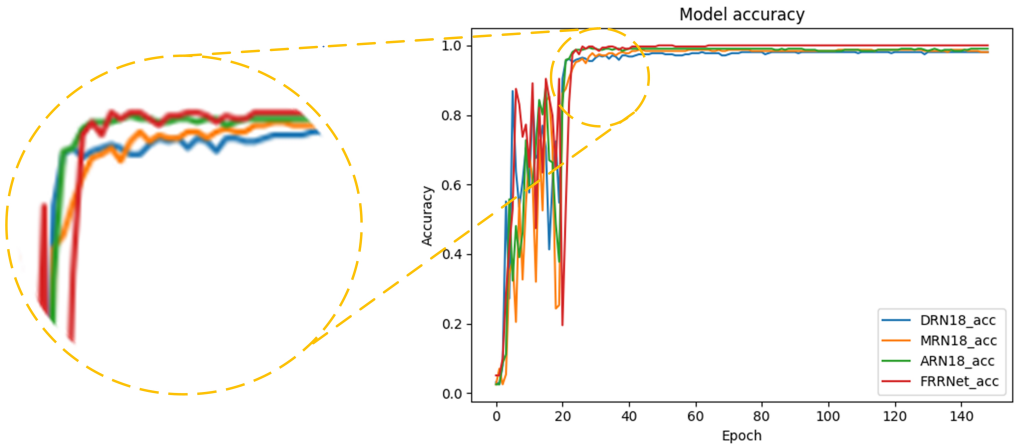

Figure 8. Network model training process demonstration in the MIT-BIH dataset: Comparison of accuracy convergence.

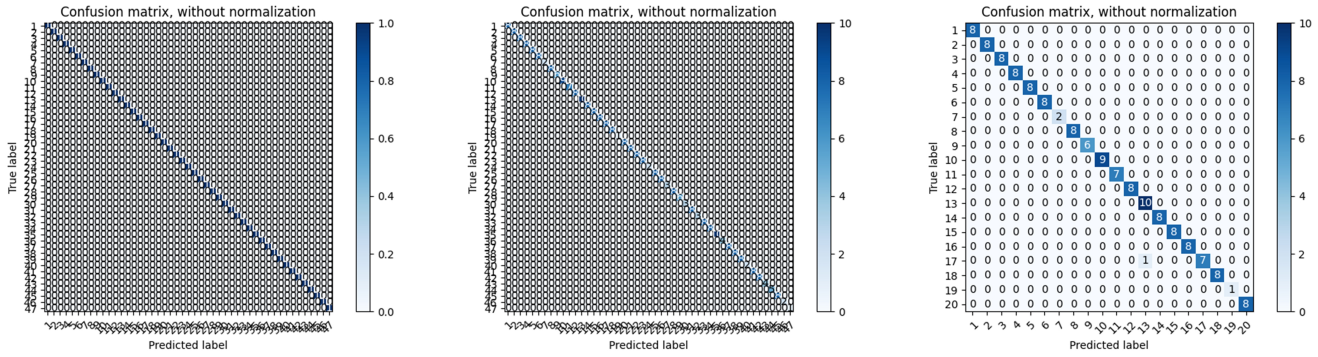

(**a**) (**b**) (**c**)

Figure 9. Identification matrix: (**a**) Testing matrix of Group 1 of FRRNet (47 subjects); (**b**) Testing matrix of Group2 of FRRNet (47 subjects); (**c**) Testing matrix of Group 2 of FRRNet (20 subjects).

4.2. Identification Results Based on the CinC_2017 Dataset

For Group 1 of the testing set, Acc, Sen and Pre of the FRRNet model proposed in this paper achieved 91.95%, 91.95% and 90.23%, respectively, and F_1 was 0.9108. Compared with the models using direct down-sampling, MP and AP, Acc was improved by 16.09%, 3.44% and 6.89%, respectively. Sen was improved by 16.09%, 3.44% and 6.89%, respectively. Pre was improved by 22.89%, 4.02% and 5.17%, respectively, and F_1 was improved by 0.1973, 0.0374 and 0.0793, respectively. For Group 2 of the testing set, Acc was 93.51%, Sen was 91.57% and Pre was 91.98%, and F_1 was 0.9177. Compared with the models using

the direct down-sampling, MP and AP, Acc was improved by 16.86%, 3.03% and 6.06%, respectively. Sen was improved by 15.6%, 1.82% and 7.65%, respectively. Pre was improved by 19.6%, 3.83% and 4.54%, respectively, and F_1 was improved by 0.1764, 0.0283 and 0.0613, respectively, as shown in Table 8. From the accuracy diagram, it can be seen that the model proposed in this paper tends to stabilise faster than the ARN18 and MRN18 models, as shown in Figure 10. The model proposed in this paper performed well on the two groups of testing sets of 50 and 87 subjects selected from the CinC_2017 dataset, and for 50 subjects, Acc was 94.52%, Sen 93.15% and Pre 92.18%, and F_1 was 0.9266. The increase in the number of subjects led to a slight decrease in the recognition accuracy, as shown in Table 9. A matrix of the results for each type of identification is shown in Figure 11. In summary, the model proposed in this paper has good performance in terms of faster convergence, higher accuracy, better robustness and less impact on accuracy when increasing the dataset on the CinC_2017 dataset.

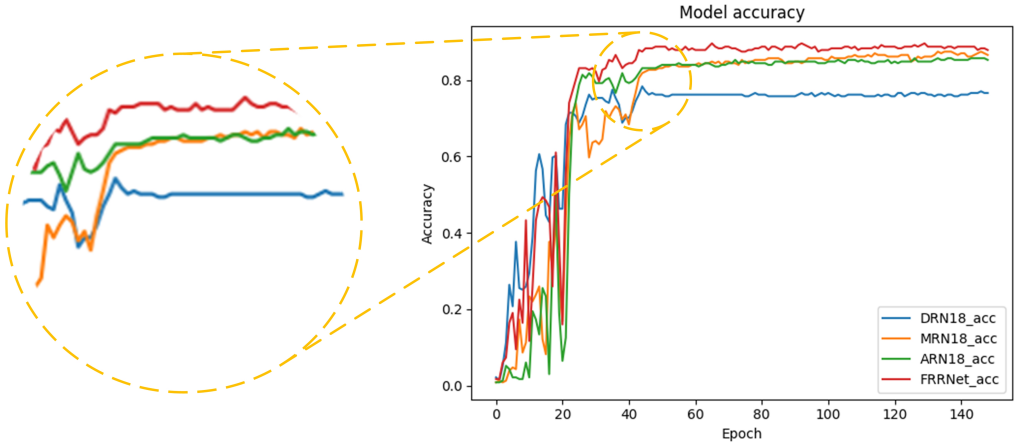

Figure 10. Network model training process demonstration in the CinC_2017 dataset: Comparison of accuracy convergence.

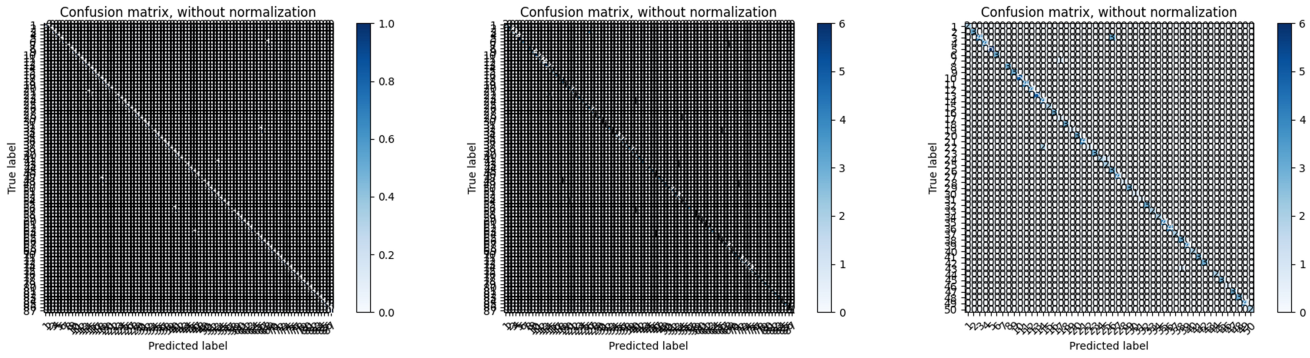

(**a**) (**b**) (**c**)

Figure 11. Identification matrix: (**a**) Testing matrix of Group 1 of FRRNet (87 subjects); (**b**) Testing matrix of Group2 of FRRNet (87 subjects); (**c**) Testing matrix of Group 2 of FRRNet (50 subjects).

Table 8. Identification accuracy results.

Model	Set	Acc	Sen	Pre	F_1	Set	Acc	Sen	Pre	F_1
DRN18	Group 1	75.86%	75.86%	67.34%	0.7135	Group 2	76.65%	75.96%	72.38%	0.7413
MRN18	Group 1	88.51%	88.51%	86.21%	0.8734	Group 2	90.48%	89.75%	88.15%	0.8894
ARN18	Group 1	85.06%	85.06%	81.32%	0.8315	Group 2	87.45%	83.92%	87.44%	0.8564
FRRNet	Group 1	**91.95%**	**91.95%**	**90.23%**	**0.9108**	Group 2	**93.51%**	**91.57%**	**91.98%**	**0.9177**

Table 9. Comparison of identification results for 50 and 87 subjects.

Number of Subjects	Acc	Sen	Pre	F_1
50	94.52%	93.15%	92.18%	0.9266
87	93.51%	91.57%	91.98%	0.9177

4.3. Identification Results Based on Group 3

For Group 3, Acc, Sen and Pre of the FRRNet model proposed in this paper achieved 98.97%, 97.50% and 99.44%, respectively, and F_1 was 0.9846, with only one ECG signal sequence recognition error. Compared with the models using direct down-sampling, MP and AP, Acc was improved by 5.16%, 1.03% and 2.06%, respectively. Sen was improved by 9.58%, 1.67% and 4.17%, respectively. Pre was improved by 10.3%, 2.94% and 3.5%, respectively, and F_1 was improved by 0.1221, 0.023 and 0.0384, respectively, as shown in Table 10. The recognition accuracy and the matrix of the FRRNet model recognition result are shown in Figure 12. To sum up, the model proposed in this paper can still retain good recognition results when the proportion of normal ECG signals is large.

Table 10. Identification accuracy results.

Model	Set	Acc	Sen	Pre	F_1
DRN18	Group 3	93.81%	87.92%	89.14%	0.8625
MRN18	Group 3	97.94%	95.83%	96.50%	0.9616
ARN18	Group 3	96.91%	93.33%	95.94%	0.9462
FRRNet	Group 3	**98.98%**	**97.50%**	**99.44%**	**0.9846**

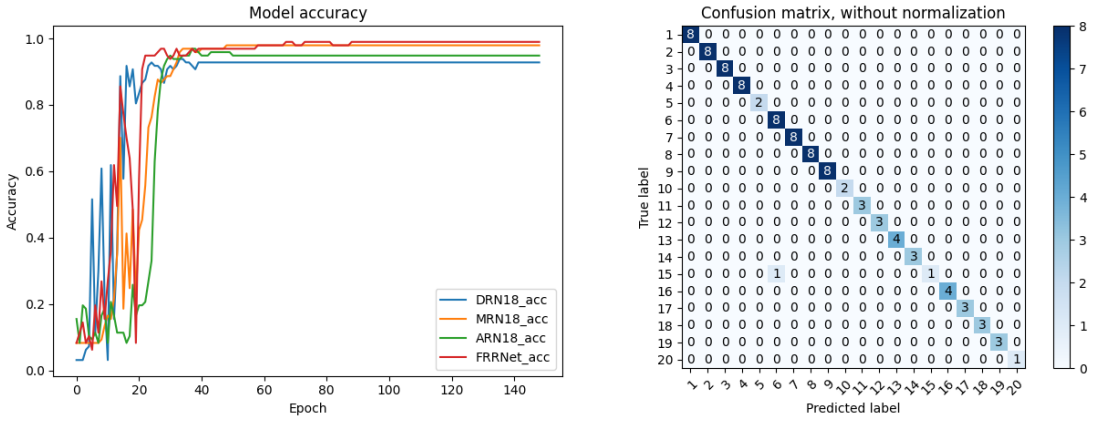

(**a**) (**b**)

Figure 12. (**a**) Comparison of the recognition accuracy of network models; (**b**) Testing matrix of Group 3 of FRRNet (20 subjects).

5. Conclusions

For Group 1 of the testing set of the MIT-BIH dataset, compared with the models using the direct down-sampling, MP and AP, the improved network model FRRNet proposed in this paper improved the accuracy by 4.26%, 2.13% and 4.26%, respectively. For Group 2 of the testing set of the MIT-BIH dataset, compared with the models using the direct down-sampling, MP and AP, the FRRNet model improved the accuracy by 1.6%, 1.28% and 4.26%, respectively. The proposed model did not decrease the recognition accuracy with the increase in subjects for the testing set, and the FRRNet model improved the recognition accuracy by 0.7–5% compared with other models.

For Group 1 of the testing set of the CinC_2017 dataset, compared with the models using the direct down-sampling, MP and AP, the FRRNet improved the accuracy by 16.09%, 3.44% and 6.89%, respectively. For Group 2 of the testing set of the CinC_2017 dataset,

compared with the models using the direct down-sampling, MP and AP, the FRRNet model improved the accuracy by 16.86%, 3.03% and 6.06%, respectively. The FRRNet model performed well on the two groups of testing sets of 50 and 87 subjects selected from the CinC_2017 dataset, with the recognition accuracy of 94.52% and 93.51%, respectively. The slight decrease in recognition accuracy was due to the increase in the number of subjects.

For Group 3, compared with the models using direct down-sampling, MP and AP, the FRRNet improved the accuracy by 5.16%, 1.03% and 2.06%, respectively, with only one ECG signal sequence misidentification.

From the experimental results, the following could be concluded. (1) The FRRNet model proposed in this paper, to some extent, solved the limitations of the models using direct down-sampling, MP and AP. (2) The FRRNet model improved the transmission of the network model features and enhanced the feature reuse. (3) The FRRNet model improved the accuracy, robustness and generalization ability of the original model. (4) The FRRNet model system performance fluctuated only slightly as the number of subjects increased. Therefore, the experimental results showed that the proposed model FRRNet was able to meet the practical requirements and could be used in real devices to provide safe and reliable biometric systems.

The recognition accuracy of the model proposed in this paper under the CinC_2017 dataset was relatively low. Part of the reason might be that the methods used for data preprocessing were relatively simple, resulting in poor preprocessing results. Future research will involve studying the methods of ECG pre-processing to further improve the performance of the model.

Author Contributions: Conceptualization, Z.Y. and L.L.; methodology, L.L.; software, L.L.; validation, L.L.; resources, L.L.; data curation, L.L.; writing—original draft preparation, L.L.; writing—review and editing, Z.Y., N.L. and J.T.; supervision, Z.Y. and N.L.; funding acquisition, Z.Y. All authors have read and agreed to the published version of the manuscript.

Funding: This work was supported in part by Shannxi Key Research and Development Plan (2021GY-318,2022GY-182); National Natural Science Foundation of China (52177193); China Scholarship Council (CSC) State Scholarship Fund International Clean Energy Talent Project (Grant No.: [2018]5046, [2019]157).

Informed Consent Statement: Informed consent was obtained from all subjects involved in the study.

Data Availability Statement: 'The MIT-BIH dataset' at https://archive.physionet.org/physiobank/database/html/mitdbdir/intro.htm#analog (accessed on 20 December 2021). 'The PhysioNet/ Computing in Cardiology Challenge 2017' at https://physionet.org/content/challenge-2017/1.0.0/ (accessed on 20 December 2021).

Conflicts of Interest: The authors declare no conflict of interest.

References

1. Jalali, A.; Mallipeddi, R.; Lee, M. Sensitive deep convolutional neural network for face recognition at large standoffs with small dataset. *Expert Syst. Appl.* **2017**, *87*, 304–315. [CrossRef]
2. Yu, Y.F.; Dai, D.Q.; Ren, C.X.; Huang, K.K. Discriminative multi-scale sparse coding for single-sample face recognition with occlusion. *Pattern Recognit.* **2017**, *66*, 302–312. [CrossRef]
3. Yang, W.; Wang, S.; Hu, J.; Zheng, G.; Valli, C. A fingerprint and finger-vein based cancelable multi-biometric system. *Pattern Recognit.* **2018**, *78*, 242–251. [CrossRef]
4. Lin, C.-H.; Chen, J.-L.; Tseng, C.Y. Optical sensor measurement and biometric-based fractal pattern classifier for fingerprint recognition. *Expert Syst. Appl.* **2011**, *38*, 5081–5089. [CrossRef]
5. Umer, S.; Sardar, A.; Dhara, B.C.; Rout, R.K.; Pandey, H.M. Person identification using fusion of iris and periocular deep features. *Neural Netw.* **2020**, *122*, 407–419. [CrossRef] [PubMed]
6. Varkarakis, V.; Bazrafkan, S.; Corcoran, P. Deep neural network and data augmentation methodology for off-axis iris segmentation in wearable headsets. *Neural Netw.* **2020**, *121*, 101–121. [CrossRef] [PubMed]
7. Huang, Z.; Siniscalchi, S.M.; Lee, C.-H. Hierarchical Bayesian combination of plug-in maximum a posteriori decoders in deep neural networks-based speech recognition and speaker adaptation. *Pattern Recognit. Lett.* **2017**, *98*, 1–7. [CrossRef]
8. Chirillo, J.; Blaul, S. *Implementing Biometric Security*; Hungry Minds, Incorporated: New York, NY, USA, 2003.

9. International Organization for Standardization. *Information Technology—Biometric Presentation Attack Detection—Part 1: Framework*; ISO: Geneva, Switzerland, 2016.
10. Wu, S.-C.; Hung, P.-L.; Swindlehurst, A.L. ECG Biometric Recognition: Unlinkability, Irreversibility, and Security. *IEEE Internet Things J.* **2020**, *8*, 487–500. [CrossRef]
11. Islam, M.S.; Alajlan, N.; Bazi, Y.; Hichri, H.S. HBS: A novel biometric feature based on heartbeat morphology. *IEEE Trans. Inf. Technol. Biomed.* **2012**, *16*, 445–453. [CrossRef]
12. Liu, J.; Yin, L.; He, C.; Wen, B.; Hong, X.; Li, Y. A multiscale autoregressive model-based electrocardiogram identification method. *IEEE Access* **2018**, *6*, 18251–18263. [CrossRef]
13. AlDuwaile, D.A.; Islam, M.S. Using Convolutional Neural Network and a Single Heartbeat for ECG Biometric Recognition. *Entropy* **2021**, *23*, 733. [CrossRef] [PubMed]
14. Khan, M.U.; Aziz, S.; Iqtidar, K.; Saud, A.; Azhar, Z. Biometric Authentication System Based on Electrocardiogram (ECG). In Proceedings of the 2019 13th International Conference on Mathematics, Actuarial Science, Computer Science and Statistics (MACS), Karachi, Pakistan, 14–15 December 2019.
15. Barros, A.; Resque, P.; Almeida, J.; Mota, R.; Oliveira, H.; Rosário, D.; Cerqueira, E. Data improvement model based on ECG biometric for user authentication and identification. *Sensors* **2020**, *20*, 2920. [CrossRef] [PubMed]
16. Israel, S.A.; Irvine, J.M.; Cheng, A.; Wiederhold, M.D.; Wiederhold, B.K. ECG to identify individuals. *Pattern Recognit.* **2005**, *38*, 133–142. [CrossRef]
17. Lin, S.L.; Chen, C.K.; Lin, C.L.; Yang, W.C.; Chiang, C.T. Individual identification based on chaotic electrocardiogram signals during muscular exercise. *IET Biom.* **2014**, *3*, 257–266. [CrossRef]
18. Belgacem, N.; Nait-Ali, A.; Fournier, R.; Bereksi-Reguig, F. ECG based human authentication using wavelets and random forests. *Int. J. Cryptogr. Inf. Secur. (IJCIS)* **2012**, *2*, 1–11. [CrossRef]
19. Zokaee, S.; Faez, K. Human identification based on ECG and palmprint. *Int. J. Electr. Comput. Eng.* **2012**, *2*, 261. [CrossRef]
20. El_Rahman, S.A. Multimodal biometric systems based on different fusion levels of ECG and fingerprint using different classifiers. *Soft Comput.* **2020**, *24*, 12599–12632. [CrossRef]
21. Belo, D.; Bento, N.; Silva, H.; Fred, A.; Gamboa, H. ECG Biometrics Using Deep Learning and Relative Score Threshold Classification. *Sensors* **2020**, *20*, 4078. [CrossRef] [PubMed]
22. Liu, X.; Si, Y.; Yang, W. A Novel Two-Level Fusion Feature for Mixed ECG Identity Recognition. *Electronics* **2021**, *10*, 2052. [CrossRef]
23. Dang, H.; Yue, Y.; Xiong, D.; Zhou, X.; Xu, X.; Tao, X. A Deep Biometric Recognition and Diagnosis Network With Residual Learning for Arrhythmia Screening Using Electrocardiogram Recordings. *IEEE Access* **2020**, *8*, 153436–153454. [CrossRef]
24. Hammad, M.; Pławiak, P.; Wang, K.; Acharya, U.R. ResNet-Attention model for human authentication using ECG signals. *Expert Syst.* **2021**, *38*, E12547. [CrossRef]
25. Yaacoubi, C.; Besrour, R.; Lachiri, Z. A multimodal biometric identification system based on ECG and PPG signals. In Proceedings of the 2nd International Conference on Digital Tools & Uses Congress, Hammamet, Tunisia, 15–17 October 2020.
26. Zhang, Y.; Xiao, Z.; Guo, Z.; Wang, Z. ECG-based personal recognition using a convolutional neural network. *Pattern Recognit. Lett.* **2019**, *125*, 668–676. [CrossRef]
27. Srivastva, R.; Singh, A.; Singh, Y.N. PlexNet: A fast and robust ECG biometric system for human recognition. *Inf. Sci.* **2021**, *558*, 208–228. [CrossRef]
28. Harvard-MIT Division of Health Sciences and Technology Biomedical Engineering Center. MIT-BIH Arrhythmia Database Directory. Available online: https://archive.physionet.org/physiobank/database/html/mitdbdir/intro.htm#analog (accessed on 24 June 2010).
29. Clifford, G.D.; Liu, C.; Moody, B.; Li-wei, H.L.; Silva, I.; Li, Q.; Johnson, A.E.; Mark, R.G. AF classification from a short single lead ECG recording: The PhysioNet/computing in cardiology challenge 2017. In Proceedings of the 2017 Computing in Cardiology (CinC), Rennes, France, 24–27 September 2017.
30. He, K.; Zhang, X.; Ren, S.; Sun, J. Deep residual learning for image recognition. In Proceedings of the IEEE Conference on Computer Vision and Pattern Recognition, Las Vegas, NV, USA, 27–30 June 2016.
31. Martis, R.J.; Acharya, U.R.; Min, L.C. ECG beat classification using PCA, LDA, ICA and discrete wavelet transform. *Biomed. Signal Process. Control* **2013**, *8*, 437–448. [CrossRef]
32. Martis, R.J.; Acharya, U.R.; Adeli, H.; Prasad, H.; Tan, J.H.; Chua, K.C.; Too, C.L.; Yeo, S.W.J.; Tong, L. Computer aided diagnosis of atrial arrhythmia using dimensionality reduction methods on transform domain representation. *Biomed. Signal Process. Control* **2014**, *13*, 295–305. [CrossRef]
33. Dewangan, N.K.; Shukla, S.P. ECG arrhythmia classification using discrete wavelet transform and artificial neural network. In Proceedings of the 2016 IEEE International Conference on Recent Trends in Electronics, Information & Communication Technology (RTEICT), Bengaluru, India, 20–21 May 2016.
34. Lee, J.; Jeong, K.; Yoon, J.; Lee, M. A simple real-time QRS detection algorithm. In Proceedings of the 18th Annual International Conference of the IEEE Engineering in Medicine and Biology Society, Amsterdam, The Netherlands, 31 October–3 November 1996.
35. Pan, J.; Tompkins, W.J. A Real-Time QRS Detection Algorithm. *IEEE Trans. Biomed. Eng.* **1985**, *3*, 230–236. [CrossRef]
26. Ding, L.-J.; Wang, X.-K.; Gao, J.; Yang, T.; Wang, F.-X.; Wang, L.-H. ECG Automatic Classification Model Based on Convolutional Neural Network. In Proceedings of the 2020 IEEE International Conference on Consumer Electronics-Taiwan (ICCE-Taiwan), Taoyuan, Taiwan, 28–30 September 2020.